JJMIE

Volume 8 Number 4, Aug 2014
ISSN 1995-6665
Pages 193 - 206

Jordan Journal of Mechanical and Industrial Engineering

# Static Bending Behavior of Functionally Graded Plates Subjected to Mechanical Loading

B. SiddaRedddy[a, *] , J. Suresh Kumar[b], C. EswaraReddy[c], K. Vijaya Kumar Reddy[d]

[a]*School of Mechanical Engineering, R.G.M. College of Engineering &Technology, Nandyal, Kurnool (Dt), Andhra Pradesh, India-518 501*

[b,d]*Department of Mechanical Engineering, J.N.T.U.H. College of Engineering, J.N.T.University, Hyderabad, India.*

[c] *The School of Engineering & Technology, SPMVV, Women's University, Tirupati, Chittoor (Dt) A.P, India*

*Received 25 Jun 2013* *accepted 16 Jul 2014*

**Abstract**

This paper presents analytical formulations and solutions for the bending behavior of simply supported functionally graded plates (FGPs) using Higher Order Shear Deformation Theory (HSDT) without enforcing zero transverse shear stresses on the top and bottom surfaces of the plate. It does not require shear correction factors. Material properties of the plate are assumed to vary in the thickness direction according to a power law distribution interns of the volume fractions of the constituents. The governing equations of motion and boundary conditions are derived using the principle of virtual work. Solutions are obtained for FGPs in closed-form using Navier's technique. The results of deflections and stresses are presented for simply supported boundary conditions. The present numerical results are compared with the available solutions in the literature for deflections and stresses, from which it can be concluded that the proposed theory results are very close agreement to the published ones. After validating the present theory results for FGM plates, the effect of side-to-thickness ratio, aspect ratio, modulus ratio, the volume fraction exponent,and through-the-thickness on the deflections and stresses are studied. The shear deformation effect and inhomogeneities played a greater role in estimating the deflctions and stress distribution in the functionally graded material plates.



**Keywords***: Static Bending Behavior, Functionally Graded Plates, Power Law, HSDT, Navier's Method*.

## 1. Introduction

Laminated Composite materials are particularly attractive to aviation and aerospace applications because of their exceptional strength and stiffness-to-density ratios and superior physical properties. However, the sudden change in material properties across the interface between discrete materials can result in large interlaminar stresses leading to delamination. Furthermore, large plastic deformations at the interfaces may trigger the initiation and propagation of cracks in the material [1]. One way to overcome these adverse effects is to employ functionally graded materials in which the material properties are continually varied through the thickness direction by mixing two different materials. This is achieved by gradually changing the volume fraction of the constituent materials usually in the thickness direction only.

In the past, researchers on plates have received great attention and a variety of plate theories have been proposed to study the mechanical behavior of FGM plates. In particular, knowledge pertaining to static analysis is essential for optimal design of structures. For example, our numerical results clearly show that one could achieve an optimal design for FGM plates with a suitable power law index "*n*". It is useful to present some developments in plate theory. The Classical Laminate Plate Theory (CLPT) [2], which is an extension of the Classical Plate Theory (CPT), provides acceptable results only for the analysis of thin plates and neglects the transverse shear effects. However, for moderately thick plates, CPT underpredicts deflections and overpredicts buckling loads and natural frequencies. The First-order Shear Deformation Theories (FSDTs) are based on Reissner's [3] and Mindlin's [4] accounts for the transverse shear deformation effect by means of a linear variation of in-plane displacements and stresses through the thickness of the plate, but requires a correction factor to satisfy the free transverse shear stress conditions on the top and bottom surfaces of the plate. Although, the FSDT provides a sufficiently accurate description of response for thin to moderately thick plates, it is not convenient to use due to difficulty with determination of the correct value of shear correction factor [5]. In order to overcome the limitations of FSDT, many HSDTs were developed; they involved higher order terms in Taylors expansions of the displacements in the

* Corresponding author. e-mail: bsrrgmcet@gmail.com.

thickness coordinate, notable among them are Reddy [6], Zenkour [7-9], Kant and Co-workers [10-15], Kadkhodayan [16], Matsunaga [17,18], Xiang [19] and Ferreira [20]. A good literature review of these theories is available in Refs. [21-23]. Neves *et al.* [20, 24] derived a Higher-order Shear Deformation Theory (HSDT) for modeling of functionally graded material plates and focused on the thickness stretching issue on the static, free vibration, and buckling analysis of FGM plates by a meshless technique. They used the virtual work principle of displacements under Carrera's Unified Formulation (CUF) to obtain the governing equations and boundary conditions. The bending and Eigen problems are solved by collocation with radial basis functions. Mechab *et al.* [25] developed a two-variable refined plate theory to the bending analysis of functionally graded plates. Mantari and Soares [26] used the new trigonometric higher order shear deformation theory with stretching effect to develop the analytical solutions for static analysis of functionally graded materials. They employed the virtual work principle to derive the governing equations of motion and boundary conditions. The bi-sinusoidal load in the transverse direction is applied to the simply supported FGM plate to obtain the Navier-type solution.

Birman and Byrd [28] presented a review of the principle developments in FGMs on the recent work published since 2000 in diverse areas relevant to various aspects of the theory and applications of FGM that include homogenization of particulate FGM, heat transfer issues, stress, stability and dynamic analyses, testing, manufacturing and design, applications, and fracture.

Reddy [29] developed analytical solutions and finite element models based on third order shear deformation plate theory to analyze the isotropic functionally graded rectangular plates accounting for the thermo-mechanical coupling, time dependency, and the von Kármán-type geometric non-linearity. He assumed that the material properties vary according to power-law distribution in terms of volume fractions of the constituents.

Cheng and Batra [30-32] used a third order shear deformation plate theory to establish the relationships between its deflections predicted by third order and higher order shear deformation theories and that given by the classical Kirchhoff plate theory. They also used the third order theory to study the buckling and steady state vibrations of a simply supported functionally gradient isotropic polygonal plate resting on a Winkler Pasternak elastic foundation and subjected to uniform in-plane hydrostatic loads. They assumed that the Young's modulus and the Poisson ratio of the material of the plate vary only in the thickness direction and also considered the rotary inertia effects. The same authors used asymptotic expansion method to study three-dimensional mechanical deformations of an isotropic linear thermo-elastic elliptic plate, and the deformations due to thermal loads are straightforwardly found.

Gasik *et al.* [33] optimized the symmetric FGM plates and disks during sintering, using computer simulation to minimize the functionally graded material distortion, to avoid cracks and to generate an optimum residual stress distribution considering the processing parameters such as green density, particle size and composition profiles.

Batra and Love [34] studied the initiation and propagation of adiabatic shear bands in FGMs deformed at high strain rates in plane-strain tension.

Qian *et al.* [35] used meshless local Petrov–Galerkin (MLPG) Method to analyze plane strain static thermoelastic deformations of a simply supported functionally graded (FG) plate. They concluded that the number of nodes required to obtain an accurate solution for a FG plate is considerably more than that needed for a homogeneous plate.

Gilhooley *et al.* [36] used a meshless local Petrov–Galerkin (MLPG) method, and a Higher-Order Shear and Normal Deformable Plate Theory (HOSNDPT) to analyze infinitesimal deformations of a functionally graded thick elastic plate. They employed multiquadrics and thin plate spline radial basis functions for constructing the trail solutions, while a fourth-order spline function is used as the weight/test function over a local sub domain. They used Mori–Tanaka homogenization technique to compute the effective material properties.

Talha and Singh [37] developed the theoretical formulations based on higher order shear deformation theory with a considerable amendment in the transverse displacement using the finite element method to analyze the thermo-mechanical deformation behavior of shear deformable FGM plates.

Daouadji *et al.* [38] presented a theoretical formulation, Navier's solutions of rectangular plates based on a new higher order shear deformation model to study the static response of FG plates enforcing traction-free boundary conditions on plate surfaces. They also studied the effect of ceramic volume fraction, volume fractions profiles, aspect ratios, and length to thickness ratios on the static response of FG plates.

Xiang and Kang [39] used nth-order shear deformation theory and meshless global collocation method based on the thin plate spline radial basis function to the bending analysis of functionally graded plates.

Most of the above theories do not account for transverse shear stresses on the top and bottom surfaces of the plate. This should be considered in modeling of the FGPs, because of the transverse shear stresses and strains are not zero, when the FGPs used in aerospace structures may be subjected to transverse load/pressure on either side of the plate.

In the present paper, analytical formulations and solutions for the static analysis of Functionally Graded Plates (FGPs) using Higher-Order Shear Deformation Theory (HSDT) are developed without enforcing zero transverse shear stress on the top and bottom surfaces of the plate. This does not require shear correction factors. The plate material is graded through the thickness direction. The plate's governing equations and its boundary conditions are derived by employing the principle of virtual work. Navier-type analytical solution is obtained for plates subjected to transverse sinusoidal load for simply supported boundary conditions. The present numerical results are compared with the available solutions in the literature for deflections and stresses, from which it can be concluded that the proposed theory results are very close agreement to the published ones. After validating the present theory results for FGM plates, the effect of side-to-thickness ratio, aspect ratio, modulus

ratio, the volume fraction exponent,and through-the-thickness on the deflections and stresses are studied. The shear deformation effect and inhomogeneities played a greater role in estimating the deflctions and stress distribution in the functionally graded material plates.

## 2. Theoretical Formulation

In formulating the higher-order shear deformation theory, a rectangular plate of length *a*, width *b* and thickness *h* is considered, that composed of functionally graded material through the thickness. Figure 1 shows the functionally graded material plate with the rectangular Cartesian coordinate system x, y and z. The material properties are assumed to be varied in the thickness direction only and the bright and dark areas correspond to ceramic and metal particles respectively. On the top surface (z=+h/2), the plate is composed of full ceramic and graded to the bottom surface (z=-h/2) that composed of full metal. The reference surface is the middle surface of the plate (z=0). The functionally graded material plate properties are assumed to be the function of the volume fraction of constituent materials. The functional relationship between the material property and the thickness coordinates is assumed to be [9, 29,40]:

$$P(z) = (P_t - P_b)\left(\frac{z}{h} + \frac{1}{2}\right)^n + P_b \quad (1)$$

where P denoted\s the effective material property, $P_t$, and $P_b$ denotes the property on the top and bottom surface of the plate, respectively, and *n* is the material variation parameter that dictates the material variation profile through the thickness. The effective material properties of the plate, including Young's modulus, E, density, ρ, and shear modulus, G, vary according to Eq. (1), and poisons ratio (υ) is assumed to be constant.

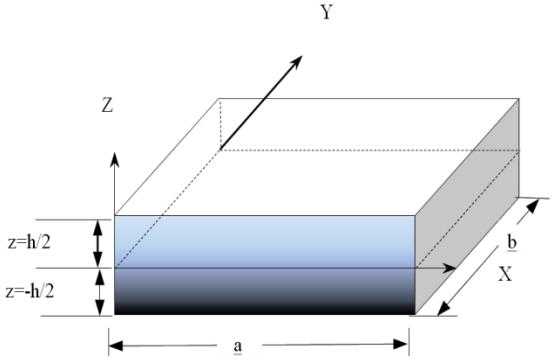


**Figure 1**.Functionally graded plate and coordinates

### *2.1. Displacement Models*

In order to approximate 3D plate problem to a 2D one, the displacement components u (x, y, z, t), v (x, y, z, t) and w (x, y, z, t) at any point in the plate are expanded in terms of the thickness coordinate. The elasticity solution indicates that the transverse shear stress varies parabolically through the plate thickness. This requires the use of a displacement field, in which the in-plane displacements are expanded as cubic functions of the thickness coordinate. In addition, the transverse normal strain may vary nonlinearly through the plate thickness. A higher-order shear deformation for composite laminated plates was developed by Pandya and Kant [41]. This paper extends this theory to functionally graded material plates. The displacement field is described in the following equations:

$$\left.\begin{aligned} u(x,y,z) &= u_o(x,y) + z\theta_x(x,y) + z^2 u_o^*(x,y) \\ &+ z^3\theta_x^*(x,y) \\ v(x,y,z) &= v_o(x,y) + z\theta_y(x,y) + z^2 v_o^*(x,y) \\ &+ z^3\theta_y^*(x,y) \\ w(x,y,z) &= w_o(x,y) \end{aligned}\right\} \quad (2)$$

Where $u_o$, $v_o$, $w_o$, denote the displacements of a point (x, y) on the mid plane.

$\theta_x$, $\theta_y$ are rotations of the normal to the mid plane about y and x-axes

$u_0^*$, $v_0^*$, $\theta_x^*$, $\theta_y^*$ are the higher order deformation terms defined at the mid plane.

By substitution of displacement relations from Eq. (2) into the strain displacement equations of the classical theory of elasticity the following relations are obtained:

$$\left.\begin{aligned} \varepsilon_x &= \varepsilon_{xo} + zk_x + z^2\varepsilon_{xo}^* + z^3 k_x^* \\ \varepsilon_y &= \varepsilon_{yo} + zk_y + z^2\varepsilon_{yo}^* + z^3 k_y^* \\ \varepsilon_z &= 0 \\ \gamma_{xy} &= \varepsilon_{xyo} + zk_{xy} + z^2\varepsilon_{xyo}^* + z^3 k_{xy}^* \\ \gamma_{yz} &= \phi_y + z\varepsilon_{yzo} + z^2\phi_y^* \\ \gamma_{xz} &= \phi_x + z\varepsilon_{xzo} + z^2\phi_x^* \end{aligned}\right\} \quad (3)$$

Where

$$\varepsilon_{xo} = \frac{\partial uo}{\partial x}, \varepsilon_{yo} = \frac{\partial vo}{\partial y}$$

$$\varepsilon_{xyo} = \frac{\partial uo}{\partial y} + \frac{\partial vo}{\partial x}$$

$$k_x = \frac{\partial \theta_x}{\partial x}, \quad k_y = \frac{\partial \theta_y}{\partial y}, \quad k_{xy} = \frac{\partial \theta_x}{\partial y} + \frac{\partial \theta_y}{\partial x}$$

$$k_x^* = \frac{\partial \theta_x^*}{\partial x}, \quad k_y^* = \frac{\partial \theta_y^*}{\partial y}, \quad k_{xy}^* = \frac{\partial \theta_x^*}{\partial y} + \frac{\partial \theta_y^*}{\partial x}$$

$$\varepsilon_{xo}^* = \frac{\partial u_o^*}{\partial x}, \quad \varepsilon_{yo}^* = \frac{\partial v_o^*}{\partial y}, \quad \varepsilon_{xyo}^* = \frac{\partial u_o^*}{\partial y} + \frac{\partial v_o^*}{\partial x}$$

$$\phi_y = \theta_y + \frac{\partial wo}{\partial y}, \quad \phi_x = \theta_x + \frac{\partial wo}{\partial x}$$

$$\varepsilon_{yzo} = 2v_o^*, \ \varepsilon_{xzo} = 2u_o^*, \ \phi_y^* = 3\theta_y^*, \ \phi_x^* = 3\theta_x^*$$

### *2.2. Elastic Stress-Strain Relations*

The elastic stress-strain relations depend on which assumption of $\varepsilon_z$=0. In the case of functionally graded materials the constitutive equations can be written as:

$$\begin{Bmatrix}\sigma_x\\ \sigma_y\\ \tau_{xy}\\ \tau_{yz}\\ \tau_{xz}\end{Bmatrix}=\begin{bmatrix}Q_{11} & Q_{12} & 0 & 0 & 0\\ Q_{12} & Q_{22} & 0 & 0 & 0\\ 0 & 0 & Q_{33} & 0 & 0\\ 0 & 0 & 0 & Q_{44} & 0\\ 0 & 0 & 0 & 0 & Q_{55}\end{bmatrix}\begin{bmatrix}\varepsilon_x\\ \varepsilon_y\\ \gamma_{xy}\\ \gamma_{yz}\\ \gamma_{xz}\end{bmatrix} \quad (4)$$

Where $\sigma = (\sigma_x, \sigma_y, \tau_{xy}, \tau_{yz}, \tau_{xz})^t$ are the stresses

$\varepsilon = (\varepsilon_x, \varepsilon_y, \gamma_{xy}, \gamma_{yz}, \gamma_{xz})^t$ are the strains with respect to the axes

$Q_{ij}$'s are the plane stress reduced elastic coefficients in the plate axes that vary through the plate thickness given by:

$$Q_{11}=Q_{22}=\frac{E(Z)}{1-\upsilon^2}=\frac{(E_c-E_m)\left(\frac{z}{h}+\frac{1}{2}\right)^n+E_m}{1-\upsilon^2}$$
$$Q_{12}=Q_{21}=\upsilon Q_{11} \quad (5)$$
$$Q_{33}=Q_{44}=Q_{55}=\frac{(1-\upsilon^2)}{2(1+\upsilon)}Q_{11}$$

Where $E_c$ is the modulus of Elasticity of the ceramic material and $E_m$ is the modulus of elasticity of the metal.

### *2.3. Governing Equations of Motion*

The work, done by actual forces in moving through virtual displacements that are consistent with the geometric constraints of a body, is set to zero to obtain the equation of motion; this is known as energy principle. It is useful for: (a) deriving governing equations and the boundary conditions, and (b) obtaining approximate solutions by virtual methods.

Energy principles provide alternative means to obtain the governing equations and their solutions. In the present study, the principle of virtual work is used to derive the equations of motion for functionally graded material plates.

The governing equations of displacement model in Eq. (2) will be derived using the dynamic version of the principle of virtual displacements [42], i.e.:

$$\int_0^T (\delta U+\delta V-\delta K)\,dt=0 \quad (6)$$

Where δU = virtual strain energy

δV = virtual work done by applied forces

δK = virtual kinetic energy

δU + δV = total potential energy.

The virtual strain energy, work done and kinetic energy are given by:

$$\delta U=\int_A\left\{\int_{-h/2}^{h/2}\begin{bmatrix}\sigma_x\delta\in_x+\sigma_y\delta\in_y+\tau_{xy}\delta\gamma_{xy}\\ +\tau_{xz}\delta\gamma_{xz}+\tau_{yz}\delta\gamma_{yz}\end{bmatrix}dz\right\}dx\,dy \quad (7)$$

$$\delta V=-\int q\delta w_0\,dx\,dy \quad (8)$$

$$\delta K=\int_A\{\int_{-h/2}^{h/2}\rho_0\begin{bmatrix}\left(\dot u_0+Z\dot\theta_x+Z^2\dot u_0^{\,*}+Z^3\dot\theta_x^{\,*}\right)\\ \left(\delta\dot u_0+Z\delta\dot\theta_x+Z^2\delta\dot u_0^{\,*}+Z^3\delta\dot\theta_x^{\,*}\right)\\ +\left(\dot v_0+Z\dot\theta_y+Z^2\dot v_0^{\,*}+Z^3\dot\theta_y^{\,*}\right)\\ \left(\delta\dot v_0+Z\delta\dot\theta_y+Z^2\delta\dot v_0^{\,*}+Z^3\delta\dot\theta_y^{\,*}\right)\\ +\dot w_0\delta\dot w_0\end{bmatrix}dz\}dx\,dy \quad (9)$$

Where

q = distributed load over the surface of the plate.

$\rho_0$ = density of plate material

Substituting for δU, δV and δK in the virtual work statement in Eq. (6) and integrating through the thickness, integrating by parts and collecting the coefficients of

$$\delta u_o,\delta v_o,\delta w_o,\delta\theta_x,\delta\theta_y,\delta u_o^{\,*},\delta v_o^{\,*},\delta\theta_x^{\,*},\delta\theta_y^{\,*}$$

the following equations of motion are obtained:

$$\delta u_0:\frac{\partial N_x}{\partial x}+\frac{\partial N_{xy}}{\partial y}=I_1\ddot u_0+I_2(\ddot\theta_x)+I_3\ddot u_0^{\,*}+I_4\ddot\theta_x^{\,*}$$

$$\delta v_0:\frac{\partial N_y}{\partial y}+\frac{\partial N_{xy}}{\partial x}=I_1\ddot v_0+I_2(\ddot\theta_y)+I_3\ddot v_0^{\,*}+I_4\ddot\theta_y^{\,*}$$

$$\delta w_0:\frac{\partial Q_x}{\partial x}+\frac{\partial Q_y}{\partial y}+q=I_1\ddot w_0$$

$$\delta\theta_x:\frac{\partial M_x}{\partial x}+\frac{\partial M_{xy}}{\partial y}-Q_x=I_2\ddot u_0+I_3(\ddot\theta_x)+I_4\ddot u_0^{\,*}+I_5\ddot\theta_x^{\,*}$$

$$\delta\theta_y:\frac{\partial M_y}{\partial y}+\frac{\partial M_{xy}}{\partial x}-Q_y=I_2\ddot v_0+I_3(\ddot\theta)_y+I_4\ddot v_0^{\,*}+I_5\ddot\theta_y^{\,*}$$

$$\delta u_0^{\,*}:\frac{\partial N_x^{\,*}}{\partial x}+\frac{\partial N_{xy}^{\,*}}{\partial y}-2S_x=I_3\ddot u_0+I_4(\ddot\theta_x)+I_5\ddot u_0^{\,*}+I_6\ddot\theta_x^{\,*}$$

$$\delta v_0^{\,*}:\frac{\partial N_y^{\,*}}{\partial y}+\frac{\partial N_{xy}^{\,*}}{\partial x}-2S_y=I_3\ddot v_0+I_4(\ddot\theta)_y+I_5\ddot v_0^{\,*}+I_6\ddot\theta_y^{\,*}$$

$$\delta\theta_x^{\,*}:\frac{\partial M_x^{\,*}}{\partial x}+\frac{\partial M_{xy}^{\,*}}{\partial y}-3\,Q_x^{\,*}=I_4\ddot u_0+I_5(\ddot\theta_x)+I_6\ddot u_0^{\,*}+I_7\ddot\theta_x^{\,*}$$

$$\delta\theta_y^{\,*}:\frac{\partial M_y^{\,*}}{\partial y}+\frac{\partial M_{xy}^{\,*}}{\partial x}-3Q_y^{\,*}=$$
$$I_4\ddot v_0+I_5(\ddot\theta_y)+I_6\ddot v_0^{\,*}+I_7\ddot\theta_y^{\,*} \quad (10)$$

Where the force and moment resultants are defined as:

$$\begin{Bmatrix}N_x & | & N_x^*\\ N_y & | & N_y^*\\ N_{xy} & | & N_{xy}^*\end{Bmatrix}=\sum_{L=1}^{n}\int_{\frac{-h}{2}}^{\frac{h}{2}}\begin{Bmatrix}\sigma_x\\ \sigma_y\\ \tau_{xy}\end{Bmatrix}\left[1\mid z^2\right]dz \quad (11)$$

$$\begin{Bmatrix} M_x & | & M_x^* \\ M_y & | & M_y^* \\ M_{xy} & | & M_{xy}^* \end{Bmatrix} = \sum_{L=1}^{n} \int_{\frac{-h}{2}}^{\frac{h}{2}} \begin{Bmatrix} \sigma_x \\ \sigma_y \\ \tau_{xy} \end{Bmatrix} \left[ z \mid z^3 \right] dz \quad (12)$$

And the transverse force resultants and the inertias are given by:

$$\begin{Bmatrix} Q_x & | & S_x & | & Q_x^* \\ Q_y & | & S_y & | & Q_y^* \end{Bmatrix} = \sum_{L=1}^{n} \int_{\frac{-h}{2}}^{\frac{h}{2}} \begin{Bmatrix} \tau_{xz} \\ \tau_{yz} \end{Bmatrix} \left[ 1 \mid z \mid z^2 \right] dz \quad (13)$$

$$I_1, I_2, I_3, I_4, I_5, I_6, I_7 = \int_{-h/2}^{h/2} \left[ (\rho_c - \rho_m) \left( \frac{2z-h}{2h} \right)^n + \rho_m \right] \left( 1, z, z^2, z^3, z^4, z^5, z^6 \right) dz \quad (14)$$

The resultants in Equations (11)-(13) can be related to the total strains in Eq. (4) by the following matrix:

$$: \begin{Bmatrix} N \\ N^* \\ -- \\ M \\ M^* \\ -- \\ Q \\ Q^* \end{Bmatrix} = \begin{bmatrix} A & | & B & | & 0 \\ B^t & | & D_b & | & 0 \\ 0 & | & 0 & | & D_s \end{bmatrix} \begin{Bmatrix} \varepsilon_0 \\ \varepsilon_0^* \\ -- \\ K_s \\ K^* \\ -- \\ \phi \\ \phi^* \end{Bmatrix} \quad (15)$$

Where,

$$\mathrm{N} = [\mathrm{N_x}\ \mathrm{N_y}\ \mathrm{N_{xy}}]^t ;\ N^* = [\mathrm{N_x^*}\ \mathrm{N_y^*}\ \mathrm{N_{xy}^*}]^t$$

N, $N^*$ are called the in-plane force resultants

$$\mathrm{M} = [\mathrm{M_x}\ \mathrm{M_y}\ \mathrm{M_{xy}}]^t ;\ M^* = [\mathrm{M_x^*}\ \mathrm{M_y^*}\ \mathrm{M_{xy}^*}]^t$$

M, $M^*$ are called as moment resultants

$$\mathrm{Q} = [\mathrm{Q_x}\ \mathrm{Q_y}]^t ;\ Q^* = [\mathrm{S_x}\ \mathrm{S_y}\ \mathrm{Q_x^*}\ \mathrm{Q_y^*}]^t$$

Q, $Q^*$ denotes the transverse force result

$$\varepsilon_0 = [\varepsilon_{x0}\ \varepsilon_{y0}\ \varepsilon_{xy0}]^t ;\ \varepsilon_0^* = [\varepsilon_{x0}^*\ \varepsilon_{y0}^*\ \varepsilon_{xy0}^*]^t$$

$$K_s = [K_x\ K_y\ K_{xy}]^t ;\ K^* = [K_x^*\ K_y^*\ K_{xy}^*]^t$$

$$\phi = [\phi_x\ \phi_y]^t ;\ \phi^* = [\varepsilon_{xz0}\ \varepsilon_{yz0}\ \phi_x^*\ \phi_y^*]^t$$

The matrices [A], [B], [D], and [Ds] are the plate stiffness whose elements can be calculated using Eq. (4), and Eq. (11)-(13).

### 3. Analytical Solutions

Rectangular plates are generally classified by referring to the type of support used. We are here concerned with the analytical solutions of the Eq. (10) - (15) for simply supported FG plates. Exact solutions of the partial differential Eq. (10) an arbitrary domain and for general boundary conditions are difficult. Although, the Navier-type solutions can be used to validate the present higher order theory, more general boundary conditions will require solution strategies involving, e.g., boundary discontinuous double Fourier series approach.

Solution functions that completely satisfy the boundary conditions in the Equations below are assumed as follows:

$$u_0(x,y,t) = \sum_{m=1}^{\infty} \sum_{n=1}^{\infty} U_{mn} \cos \alpha x \sin \beta y; \quad 0 \le \mathrm{x} \le \mathrm{a};\ 0 \le \mathrm{y} \le \mathrm{b} \quad 16(a)$$

$$v_0(x,y,t) = \sum_{m=1}^{\infty} \sum_{n=1}^{\infty} V_{mn} \sin \alpha x \cos \beta y; \quad 0 \le \mathrm{x} \le \mathrm{a};\ 0 \le \mathrm{y} \le \mathrm{b} \quad 16(b)$$

$$w_0(x,y,t) = \sum_{m=1}^{\infty} \sum_{n=1}^{\infty} W_{mn} \sin \alpha x \sin \beta y; \quad 0 \le \mathrm{x} \le \mathrm{a};\ 0 \le \mathrm{y} \le \mathrm{b} \quad 16(c)$$

$$\theta_x(x,y,t) = \sum_{m=1}^{\infty} \sum_{n=1}^{\infty} X_{mn} \cos \alpha x \sin \beta y; \quad 0 \le \mathrm{x} \le \mathrm{a};\ 0 \le \mathrm{y} \le \mathrm{b} \quad 16(d)$$

$$\theta_y(x,y,t) = \sum_{m=1}^{\infty} \sum_{n=1}^{\infty} Y_{mn} \sin \alpha x \cos \beta y; \quad 0 \le \mathrm{x} \le \mathrm{a};\ 0 \le \mathrm{y} \le \mathrm{b} \quad 16(e)$$

$$u_0^*(x,y,t) = \sum_{m=1}^{\infty} \sum_{n=1}^{\infty} U_{mn}^* \cos \alpha x \sin \beta y; \quad 0 \le \mathrm{x} \le \mathrm{a};\ 0 \le \mathrm{y} \le \mathrm{b} \quad 16(f)$$

$$V_o^*(x,y,t) = \sum_{m=1}^{\infty} \sum_{n=1}^{\infty} V_{mn}^* \sin \alpha x \cos \beta y; \quad 0 \le \mathrm{x} \le \mathrm{a};\ 0 \le \mathrm{y} \le \mathrm{b} \quad 16(g)$$

$$\theta_x^*(x,y,t) = \sum_{m=1}^{\infty} \sum_{n=1}^{\infty} X_{mn}^* \cos \alpha x \sin \beta y; \quad 0 \le \mathrm{x} \le \mathrm{a};\ 0 \le \mathrm{y} \le \mathrm{b} \quad 16(h)$$

$$\theta_y^*(x,y,t) = \sum_{m=1}^{\infty} \sum_{n=1}^{\infty} Y_{mn}^* \sin \alpha x \cos \beta y; \quad 0 \le \mathrm{x} \le \mathrm{a};\ 0 \le \mathrm{y} \le \mathrm{b} \quad 16(i)$$

Where

$$\alpha = \frac{m\pi}{a} \text{ and } \beta = \frac{n\pi}{b}$$

The Mechanical load is expanded in double Fourier sine series as:

$$q(x,y,) = \sum_{m=1}^{\infty} \sum_{n=1}^{\infty} Q_{mn} \sin \alpha x \sin \beta y \quad (17)$$

Substituting Eq. (16a) - (16i) into Eq. (10) and collecting the coefficients we obtain:

$$[S]_{9\times 9}\begin{Bmatrix} U_{mn} \\ V_{mn} \\ W_{mn} \\ X_{mn} \\ Y_{mn} \\ U_{nm}^{*} \\ V_{mn}^{*} \\ X_{mn}^{*} \\ Y_{mn}^{*} \end{Bmatrix}_{9\times 1} = \begin{Bmatrix} 0 \\ 0 \\ Q_{mn} \\ 0 \\ 0 \\ 0 \\ 0 \\ 0 \\ 0 \end{Bmatrix}_{9\times 1} \quad (18)$$

For any fixed value of m and n. Solutions of the Eq. (18) are obtained for each m,n =1,2….as Umn, Vmn, Wmn, Xmn,Ymn.

The coefficients Umn, Vmn, Wmn, Xmn, Ymn, $U_{mn}^{*}, V_{mn}^{*}, X_{mn}^{*}, Y_{mn}^{*}$ which are used to compute $u_o, v_o, w_o, \theta_x, \theta_y, u_o^{*}, v_o^{*}, \theta_x^{*}, \theta_y^{*}$.

## 4. Results and Discussion

### *4.1. Comparative Studies*

In this section, numerical examples are presented and discussed to verify the accuracy of the present higher-order shear deformation theory in predicting the deflections and stresses of a simply supported functionally graded material plate. For numerical results, an $Al/Al_2O_3$ Plate is considered and graded from aluminum (as metal) at the bottom to alumina (as ceramic) at the top surface of the plate. The material properties adopted here are:

Aluminium Young's modulus ($E_m$): 70GPa, density($\rho_m$)= 2702 kg/m$^3$, and Poisson's ratio (υ): 0.3

Alumina Young's modulus ($E_c$): 380GPa, density ($\rho_c$)= 3800kg/m$^3$, and Poisson's ratio (υ): 0.3

For convenience, the transverse displacement, in-plane and the transverse shear stresses are presented in nondimensionalized form as:

$$\overline{w} = 10w_0\left(\frac{a}{2},\frac{b}{2}\right)\times\frac{E_c h^3}{qa^4};\ \overline{\sigma}_x = \frac{h}{aq}\sigma_x\left(\frac{a}{2},\frac{b}{2},\frac{h}{2}\right)$$

$$\overline{\sigma}_y = \frac{h}{aq}\sigma_x\left(\frac{a}{2},\frac{b}{2},\frac{h}{3}\right);\ \overline{\tau}_{xy} = \frac{h}{aq}\tau_{xy}\left(0,0,-\frac{h}{3}\right)$$

$$\overline{\tau}_{yz} = \frac{h}{aq}\tau_{yz}\left(\frac{a}{2},0,\frac{h}{6}\right);\ \overline{\tau}_{xz} = \frac{h}{aq}\tau_{xz}\left(0,\frac{b}{2},0\right)$$

and $\overline{z} = \frac{z}{h}$

In Table 1, we present results for in-plane longitudinal, normal stresses and transverse displacements for various material variation parameter *"n"* of the power law and for side-to-thickness ratios (a/h) is 10. The present results are compared with the Zenkour [9], Reddy [6], Touraiter [27] and Mechab [25].

The results from present higher-order shear deformation theory considering $\varepsilon_z$=0 are in good agreement with those from Touraiter [27] and Mechab [25] who also consider $\varepsilon_z$=0. It can also be seen that the effect of the exponent "n" of the power law on the dimensionless deflections and stresses of an FGM plate is being demonstrated in the results presented in Table 1. From Table 1, it is important to observe that as the plate becomes more and more metallic, the difference increases for maximum center deflection and maximum normal stress ($\overline{\sigma}_x$), while it decreases for normal stress ($\overline{\sigma}_y$). Also, it is noticed that the stresses for a fully ceramic plate are the same as that for a fully metal plate. This may be because of the fact that the plate is fully homogeneous at the top and bottom surface and the nondimensionalized stresses do not depend on the value of the modulus of elasticity.

Table 2 compares the deflections and transverse shear stresses in a square FG plate subjected to sinusoidal distributed load. For convenience, the transverse displacement, and the transverse shear stresses in Table 2 are presented in a nondimensionalized form as:

$$\overline{w} = w_0\left(\frac{a}{2},\frac{b}{2}\right)\times\frac{E_c}{qh};\quad \overline{\tau}_{xz} = \frac{\tau_{xz}}{q}\left(0,\frac{b}{2},0\right)$$

It can be seen that the deflections and stresses are in good agreementg with the higher order shear deformation theory [18] and refined plate theory [25]. This allows us to conclude that the developed higher order shear deformation theory is good for modelling of simply supported FGM plates. Results in Table 1 and Table 2 should serve as benchmark results for future comparisons.

**Table 1**: Comparison of Non-dimensional Central deflections and stresses in a square FG-plate subjected to sinusoidal distributed load, a/h=10.

| n | Source | $\overline{w}$ | $\overline{\sigma}_x$ | $\overline{\sigma}_y$ | $\overline{\tau}_{xy}$ | $\overline{\tau}_{yz}$ | $\overline{\tau}_{xz}$ |
|---|---|---|---|---|---|---|---|
| Ceramic | Ref.[9] | 0.2960 | 1.995500 | 1.312100 | 0.706500 | 0.213200 | 0.246200 |
| | Ref.[6] | 0.29423 | 1.989150 | 1.310350 | 0.705570 | 0.190510 | 0.237780 |
| | Ref.[27] | 0.2960 | 1.995500 | 1.312100 | 0.706500 | 0.213200 | 0.246200 |
| | Ref.[25] | 0.2961 | 1.994300 | 1.312400 | 0.706700 | 0.212100 | 0.238600 |
| | **Present** | **0.2961** | **1.99426** | **1.31238** | **0.706667** | **0.211994** | **0.238413** |
| 0.2 | Ref.[6] | 0.33767 | 2.126710 | 1.309580 | 0.667570 | 0.180450 | 0.225320 |
| | **Present** | **0.3599** | **2.259090** | **1.38728** | **0.720591** | **0.225440** | **0.242348** |
| 0.5 | Ref.[6] | 0.4407 | 2.610510 | 1.471470 | 0.666680 | 0.190710 | 0.238170 |
| | **Present** | **0.4537** | **2.61874** | **1.45902** | **0.691134** | **0.240484** | **0.243518** |
| 1 | Ref.[9] | 0.5889 | 3.087000 | 1.489400 | 0.611000 | 0.262200 | 0.246200 |
| | Ref.[6] | 0.58895 | 3.085010 | 1.489800 | 0.611110 | 0.190710 | 0.238170 |
| | Ref.[27] | 0.5889 | 3.087000 | 1.489400 | 0.611000 | 0.262200 | 0.246200 |
| | Ref.[25] | 0.5890 | 3.085000 | 1.489800 | 0.611100 | 0.260800 | 0.238600 |
| | **Present** | **0.5890** | **3.08782** | **1.49034** | **0.610704** | **0.254721** | **0.238405** |
| 2 | Ref.[9] | 0.7573 | 3.609400 | 1.395400 | 0.544100 | 0.276300 | 0.226500 |
| | Ref.[6] | 0.75747 | 3.606640 | 1.395750 | 0.544340 | 0.180700 | 0.225680 |
| | Ref.[27] | 0.7573 | 3.609400 | 1.395400 | 0.544100 | 0.276300 | 0.226500 |
| | Ref.[25] | 0.7573 | 3.606700 | 1.396000 | 0.544200 | 0.273700 | 0.218600 |
| | **Present** | **0.7578** | **3.61635** | **1.39638** | **0.543421** | **0.263908** | **0.222026** |
| 3 | Ref.[27] | 0.8377 | 3.874200 | 1.274800 | 0.552500 | 0.271500 | 0.210700 |
| | Ref.[25] | 0.8375 | 3.870900 | 1.275600 | 0.552600 | 0.267700 | 0.202400 |
| | **Present** | **0.8383** | **3.88527** | **1.27495** | **0.551783** | **0.260625** | **0.208393** |
| 4 | Ref.[27] | 0.8819 | 4.069300 | 1.178300 | 0.566700 | 0.258000 | 0.202900 |
| | Ref.[25] | 0.8816 | 4.065500 | 1.179400 | 0.566900 | 0.253700 | 0.194400 |
| | **Present** | **0.8823** | **4.08134** | **1.17786** | **0.566122** | **0.250169** | **0.201285** |
| 5 | Ref.[9] | 0.91180 | 4.248800 | 1.102900 | 0.575500 | 0.242900 | 0.201700 |
| | Ref.[6] | 0.90951 | 4.242930 | 1.105390 | 0.573680 | 0.173070 | 0.216090 |
| | Ref.[27] | 0.9118 | 4.248800 | 1.102900 | 0.575500 | 0.242900 | 0.201700 |
| | Ref.[25] | 0.9112 | 4.244700 | 1.104100 | 0.575700 | 0.238500 | 0.193000 |
| | **Present** | **0.9121** | **4.25983** | **1.1022** | **0.574958** | **0.237709** | **0.199975** |
| 6 | Ref.[27] | 0.9356 | 4.424400 | 1.041700 | 0.580300 | 0.229600 | 0.204100 |
| | Ref.[25] | 0.9352 | 4.420100 | 1.042800 | 0.580600 | 0.225500 | 0.195400 |
| | **Present** | **0.9357** | **4.43346** | **1.04095** | **0.579958** | **0.226524** | **0.202127** |
| 7 | Ref.[27] | 0.9562 | 4.597100 | 0.990300 | 0.583400 | 0.219400 | 0.208100 |
| | Ref.[25] | 0.9557 | 4.592800 | 0.991500 | 0.583600 | 0.215700 | 0.199400 |
| | **Present** | **0.9562** | **4.60395** | **0.98971** | **0.583103** | **0.217854** | **0.205747** |
| 8 | Ref.[27] | 0.9750 | 4.766100 | 0.946600 | 0.585600 | 0.212100 | 0.212400 |
| | Ref.[25] | 0.9743 | 4.761900 | 0.947700 | 0.585800 | 0.208800 | 0.203700 |
| | **Present** | **0.9749** | **4.77066** | **0.946138** | **0.585446** | **0.211753** | **0.209630** |

| n | Source | $\bar{w}$ | $\bar{\sigma}_x$ | $\bar{\sigma}_y$ | $\bar{\tau}_{xy}$ | $\bar{\tau}_{yz}$ | $\bar{\tau}_{xz}$ |
|---|---|---|---|---|---|---|---|
| 9 | Ref.[27] | 0.9925 | 4.930300 | 0.909200 | 0.587500 | 0.207200 | 0.216400 |
| | Ref.[25] | 0.9922 | 4.926100 | 0.910300 | 0.587800 | 0.204200 | 0.207800 |
| | **Present** | **0.9924** | **4.93267** | **0.908967** | **0.587472** | **0.207791** | **0.213196** |
| 10 | Ref.[27] | 1.0089 | 5.089000 | 0.877500 | 0.589400 | 0.204100 | 0.219800 |
| | Ref.[25] | 1.0085 | 5.084900 | 0.878500 | 0.589600 | 0.201400 | 0.211400 |
| | **Present** | **1.0089** | **5.08932** | **0.87743** | **0.589390** | **0.205434** | **0.216235** |
| Metal | Ref.[9] | 1.60700 | 1.995500 | 1.312100 | 0.706500 | 0.213200 | 0.246200 |
| | Ref.[6] | 1.59724 | 1.989150 | 1.310350 | 0.705570 | 0.190510 | 0.237780 |
| | Ref.[27] | 1.6070 | 1.995500 | 1.312100 | 0.706500 | 0.213200 | 0.246200 |
| | Ref.[25] | 1.6074 | 1.994300 | 1.312400 | 0.706700 | 0.212100 | 0.238600 |
| | **Present** | **1.6072** | **10.826** | **1.31238** | **0.706667** | **0.211994** | **0.238413** |

**Table 2**: Comparison of Non-dimensional Central deflections and transverse shear stress in a square FG-plate subjected to sinusoidal distributed load

| a/h | Power law index, *n* | $\bar{w}$ | | | $\bar{\tau}_{xz}$ | | |
|---|---|---|---|---|---|---|---|
| | | Ref.[18] | Ref.[25] | Present | Ref.[18] | Ref.[25] | Present |
| 5 | 0 | 20.98 | 21.46 | 21.4575 | 1.186 | 1.19 | 1.18735 |
| | 0.5 | 31.79 | 32.35 | 32.3549 | 1.209 | 1.217 | 1.21301 |
| | 1 | 41.39 | 41.8 | 41.816 | 1.184 | 1.19 | 1.18719 |
| | 4 | 65.12 | 65.06 | 65.2529 | 1.076 | 0.969 | 1.0005 |
| | 10 | 76.21 | 76.72 | 76.7671 | 1.078 | 1.053 | 1.07547 |
| 10 | 0 | 294.3 | 296.1 | 296.058 | 2.383 | 2.385 | 2.38413 |
| | 0.5 | 450.4 | 453.7 | 453.716 | 2.431 | 2.439 | 2.43518 |
| | 1 | 587.5 | 589 | 589.03 | 2.383 | 2.385 | 2.38405 |
| | 4 | 882.3 | 881.6 | 882.341 | 2.175 | 1.943 | 2.01285 |
| | 10 | 1007 | 1008.5 | 1008.92 | 2.167 | 2.113 | 2.16235 |

### *4.2. Parametric Study*

#### *4.2.1. Effect of Side-to-Thickness Ratio*

The variation of nondimensionalized displacements and stresses for various side to thickness ratios (a/h) and material variation parameter (n) for displacement model are shown in Figures 2 - 7. Figure 2 shows the variation of center deflection for various volume fraction exponents "n" and with different side-to-thickness ratios, respectively. It is observed that the deflection of FGM plate is between ceramic and metal and the deflection of metal rich plates is larger compared to ceramic rich plates, this is due to the fact that the modulus of elasticity of ceramic ($Al_2O_3$=380GPa) is higher than that of metal (Al:70GPa). Hence for FGM plates, the transverse deflection decreases as the volume fraction exponent, n, decreases, whereas it may be unchanged as the side-to-thickness ratio increases. The normal stresses increases with the increase of side-to-thickness ratio and decreases with the decrease of volume fraction exponent which can be seen in Figure 3 and Figure 4. Figures 5 - 7 show the variation of nondimensionalized shear stress for various side-to-thickness ratios and with different power-law index values. It can be seen that the longitudinal shear stress ($\bar{\tau}_{xy}$) increases with the increase of side-to-thickness ratio's and power-law index values. This is due to the decrease of the stiffness of the plate. The transversal shear stresses may be unchanged as the side-to-thickness ratio increases. The shear deformation effect is to increase the deflections and decrease the normal stresses, longitudinal and transverse shear stresses, especially for a/h≤5.

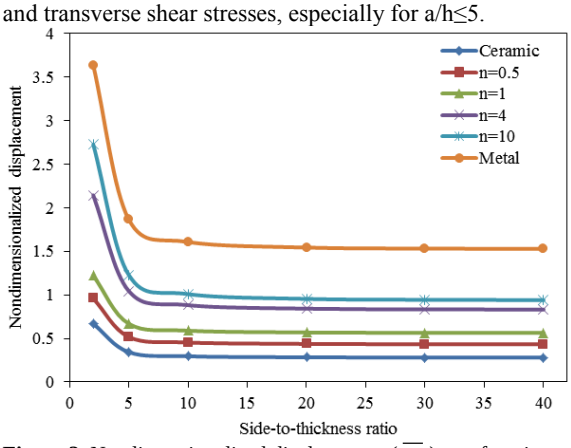


**Figure 2**. Nondimensionalized displacement ($\bar{w}$) as a function of side-to-thickness ratio (a/h) of an FGM plate for various values of power law index (n)

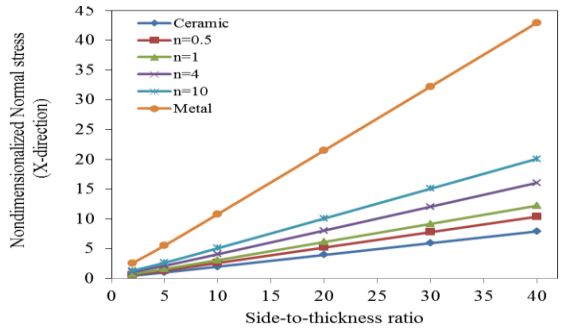


**Figure 3**. Nondimensionalized Normal stress ( $\bar{\sigma}_x$ ) as a function of side-to-thickness ratio (a/h) of an FGM plate for various values of power law index (n)

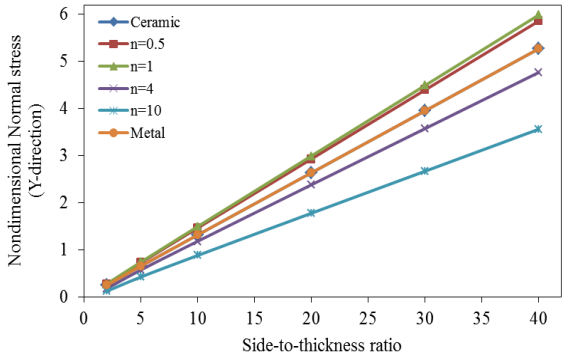


**Figure 4**. Nondimensionalized Normal stress ( $\bar{\sigma}_y$ ) as a function of side-to-thickness ratio (a/h) of an FGM plate for various values of power law index (n)

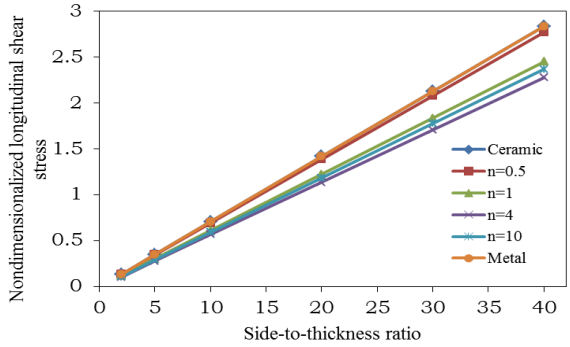


**Figure 5**: Nondimensionalized longitudinal shear stress ( $\bar{\tau}_{xy}$ ) as a function of side-to-thickness ratio (a/h) of an FGM plate for various values of power law index (n)

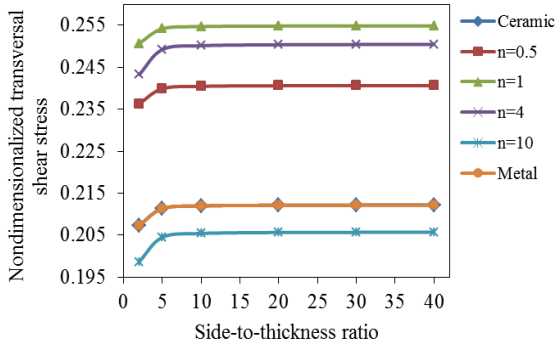


**Figure 6**: Nondimensionalized transversal shear stress ( $\bar{\tau}_{yz}$ ) as a function of side-to-thickness ratio (a/h) of an FGM plate for various values of power law index (n)

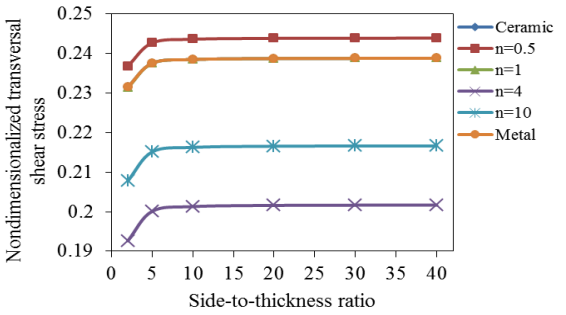


**Figure 7**: Nondimensionalized transversal shear stress ( $\bar{\tau}_{xz}$ ) as a function of side-to-thickness ratio (a/h) of an FGM plate for various values of power law index (n)

### *4.2.2. Effect of Aspect Ratio*

The effect of aspect ratios (a/b) and material variation parameter (n) for displacement model on nondimensionalized displacements and stresses are shown in Figures 8 - 13. From Figure 8 and Figure 9, it can be seen that the nondimensionalized center deflections and in-plane longitudinal stress ( $\bar{\sigma}_x$ ) decreases with the increase of aspect ratio and volume fraction exponent. The nondimensionalized displacements are higher for metallic plates and lower for ceramic plates. This is because of more stiffness for ceramics plates than metal plates. Also, it is found that the response of FGM plates is intermediate to that of the ceramic and metal homogeneous plates. The normal stress ( $\bar{\sigma}_y$ ) and the longitudinal shear stress ( $\bar{\tau}_{xy}$ ) increases with the increase of aspect ratio up to 0.5 and then decreases, this can be observed in Figure 10 and Figure 11. It is due to the increase of elastic constants, $Q_{ij}$. It can be seen from Figure 12 that transversal shear stress ( $\bar{\tau}_{yz}$ ) increases to a maximum when aspect ratio a/b=1 and power-law index=1. Further it decreases with the increase of aspect ratio. Figure 13 shows the variation of nondimensionalized transversal shear stress ( $\bar{\tau}_{xz}$ ) with the aspect ratio for different power-law index values. It is observed that the transversal shear stress ( $\bar{\tau}_{xz}$ ) decreases with the increase of aspect ratio. From Figure 8 to Figure 13, it can be seen that the effect of coupling increases as the aspect ratio increases.

### *4.2.3. Effect of Modulus Ratio*

The effect of modulus ratios ($E_m/E_c$) and material variation parameter (n) for displacement model is shown in Figures 14 - 19. Figure 14 and Figure 15 show the variation of center deflection and in-plane longitudinal stress ( $\bar{\sigma}_x$ ) with the modulus ratios and volume fraction exponent. The deflections and in-plane longitudinal stress decreases with the increase of volume fraction exponent and modulus ratios. From the figures, it is seen that maximum center deflections decrease smoothly with the decrease of volume fraction exponent, n, and metal-ceramic modulii ratio increases. This is because of the increase of the ratio of metal-ceramic modulii. The in-plane-normal stress ( $\bar{\sigma}_y$ ) and the shear stresses variation with volume fraction exponent is depicted in Figures 16 - 19. The shear stresses, $\bar{\tau}_{xy}$ , $\bar{\tau}_{xz}$ increase with the increase

of modulus ratio and maximum shear stress occurs at volume fraction exponent, n=0.2 and 0.5, respectively, while transverse shear stress, $\bar{\tau}_{yz}$ decreases with increase of volume fraction exponent.

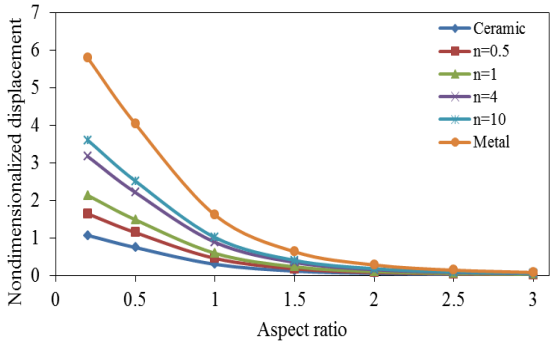


**Figure 8**: Nondimensionalized displacement ( $\bar{w}$ ) as a function of aspect ratio (a/b) of an FGM plate for various values of power law index (n)

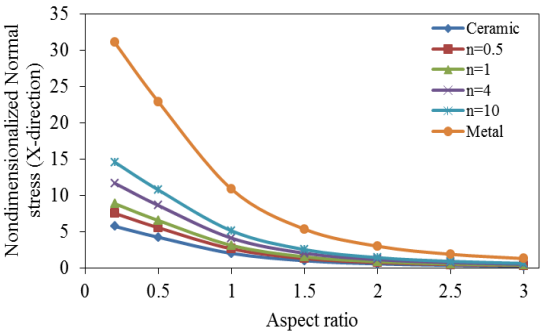


**Figure 9**: Nondimensionalized Normal stress ( $\bar{\sigma}_x$ ) as a function of aspect ratio (a/b) of an FGM plate for various values of power law index (n)

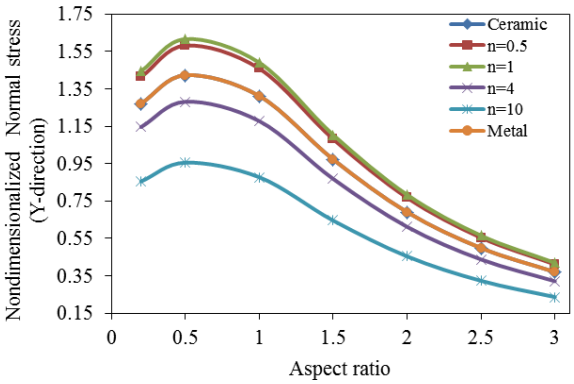


**Figure 10**: Nondimensionalized Normal stress ( $\bar{\sigma}_y$ ) as a function of aspect ratio (a/b) of an FGM plate for various values of power law index (n)

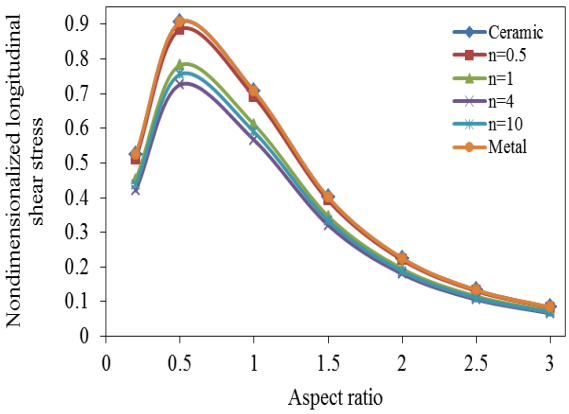


**Figure 11**: Nondimensionalized longitudinal shear stress ( $\bar{\tau}_{xy}$ ) as a function of aspect ratio (a/b) of an FGM plate for various values of power law index (n)

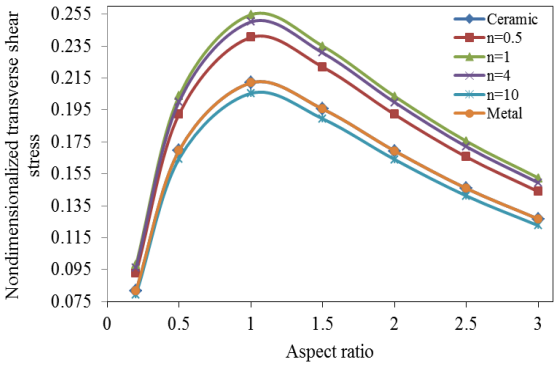


**Figure 12**: Nondimensionalized transversal shear stress ( $\bar{\tau}_{yz}$ ) as a function of aspect ratio (a/b) of an FGM plate for various values of power law index (n)

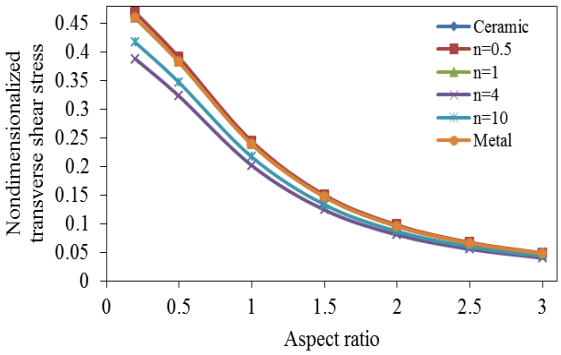


**Figure 13**: Nondimensionalized transversal shear stress ( $\bar{\tau}_{xz}$ ) as a function of aspect ratio (a/b) of an FGM plate for various values of power law index (n)

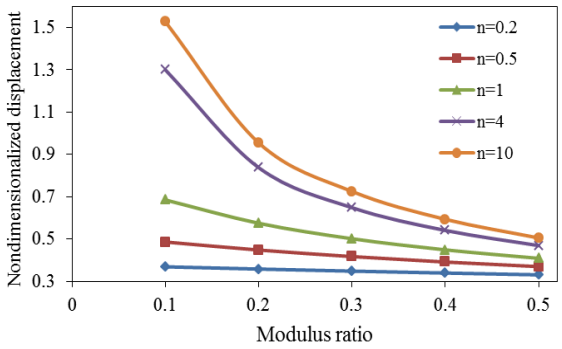


**Figure 14**: Nondimensionalized displacement ( $\overline{w}$ ) as a function of modulus ratio ($E_c/E_m$) of an FGM plate for various values of power law index (n)

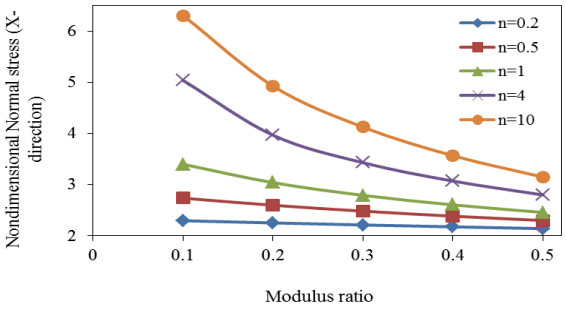


**Figure 15**: Nondimensionalized Normal stress ( $\overline{\sigma}_x$ ) as a function of modulus ratio ($E_c/E_m$) of an FGM plate for various values of power law index (n)

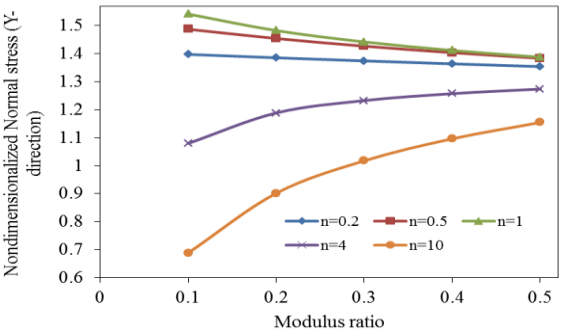


**Figure 16**: Nondimensionalized Normal stress ( $\overline{\sigma}_y$ ) as a function of modulus ratio ($E_c/E_m$) of an FGM plate for various values of power law index (n)

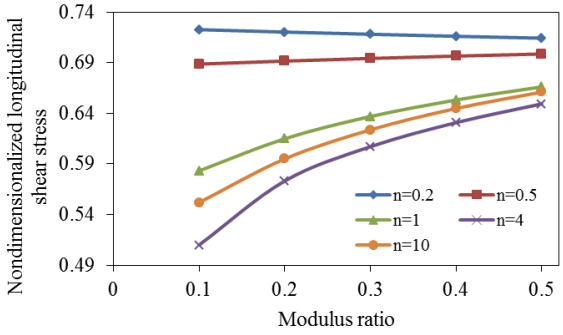


**Figure 17**: Nondimensionalized longitudinal shear stress ( $\overline{\tau}_{xy}$ ) as a function of modulus ratio ($E_c/E_m$) of an FGM plate for various values of power law index (n)

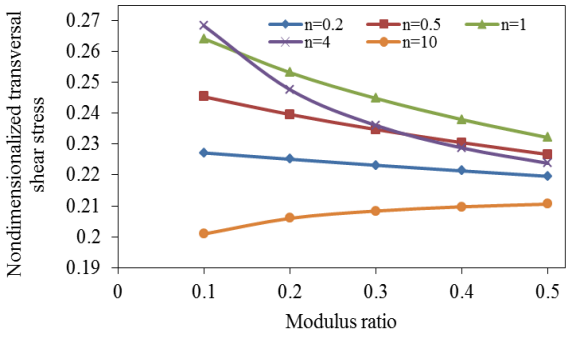


**Figure 18**: Nondimensionalized transversal shear stress ( $\overline{\tau}_{yz}$ ) as a function of modulus ratio ($E_c/E_m$) of an FGM plate for various values of power law index (n) for model

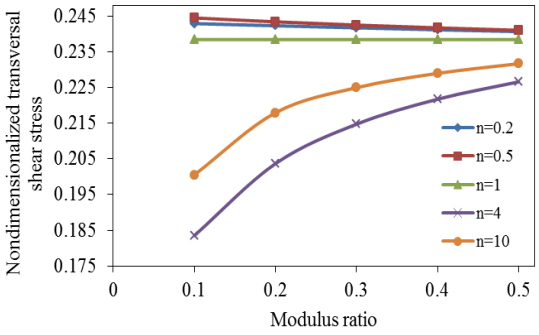


**Figure 19**: Nondimensionalized transversal shear stress ( $\overline{\tau}_{xz}$ ) as a function of modulus ratio ($E_c/E_m$) of an FGM plate for various values of power law index (n)

### *4.2.4. Variation of Stresses in Through-the-Thickness*

Figures 20 - 24 show the variation of in-plane longitudinal stress ( $\overline{\sigma}_x$ ), in-plane normal stress ( $\overline{\sigma}_y$ ), longitudinal shear stress ( $\overline{\tau}_{xy}$ ) and transversal shear stresses ( $\overline{\tau}_{yz}$ , $\overline{\tau}_{xz}$ ), respectively in the FGM plate under the sinusoidal load, for different values of power-law index values. As exhibited in Figure 20 and Figure 21, the in-plane longitudinal stress ( $\overline{\sigma}_x$ ), in-plane normal stress ( $\overline{\sigma}_y$ ), are compressive throughout the plate up to $\overline{Z} \cong 0.157$ and then become tensile afterwards. The maximum tensile stresses occur at the top surface of the plate and maximum compressive stresses occur at a point on the bottom of the plate.

Figures 22 - 24 depict the through-the-thickness distributions of the shear stresses ( $\overline{\tau}_{xy}$ $\overline{\tau}_{xy}$ , $\overline{\tau}_{xy}$ ) in the FGM plate under sinusoidal load for different volume fraction exponents. The distinction among the curves is obvious. As the strain gradients increase, the inhomogeneities play a greater role in stress distribution calculations. The through-the-thickness distributions are not parabolic and it is to be noticed that the maximum shear stress value occurs at $\overline{Z}$ =0.2 for volume fraction exponent, n=2, not at the plate center as in the case of homogeneous case.

  

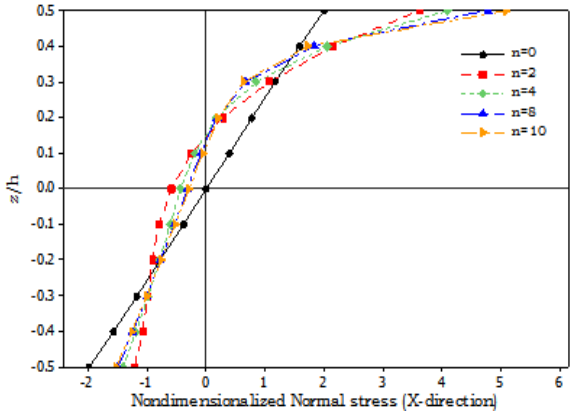


**Figure 20**: Variation of in-plane longitudinal stress ( $\overline{\sigma}_x$ ) across the thickness of an FGM plate for different power-law index, n

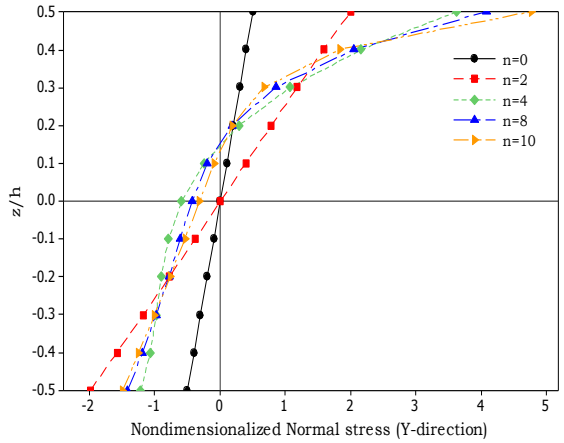


**Figure 21**:Variation of in-plane normal stress ( $\overline{\sigma}_y$ ) across the thickness of an FGM plate for different power-law index,n

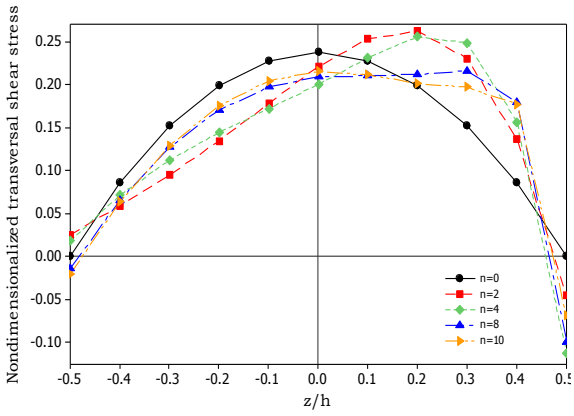


**Figure 24**:Variation of transversal shear stress ( $\overline{\tau}_{xz}$ ) across the thickness of an FGM plate for different power-law index, n

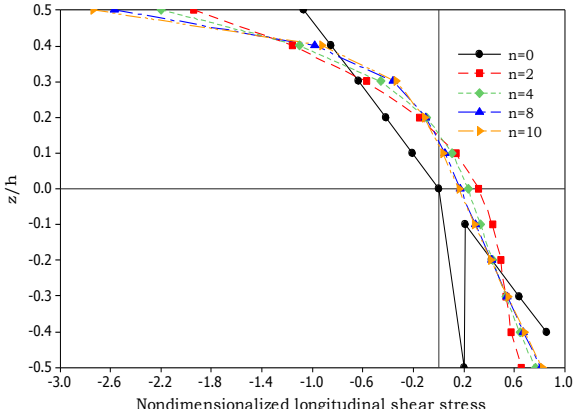


**Figure 22**:Variation of longitudinal shear stress ( $\overline{\tau}_{xy}$ ) across the thickness of an FGM plate for different power-law index, n

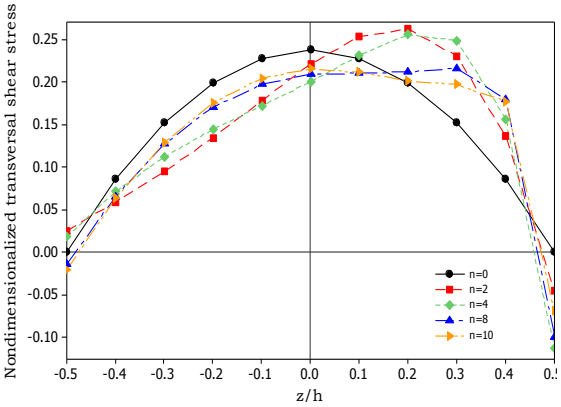


**Figure 23**:Variation of transversal shear stress ( $\overline{\tau}_{yz}$ ) across the thickness of an FGM plate for different power-law index, n

## Conclusions

A higher-order shear deformation theory was successfully developed for static bending behavior of simply supported functionally graded plates without enforcing zero transverse shear stresses on the top and bottom surfaces of the plate. This eliminated the need of shear correction factors. The material properties are assumed to vary according to power law distribution. The governing equations and boundary conditions are derived by employing the principle of virtual work. The governing equations are solved using Navier's type closed form solution, for FG plates subjected to sinusoidal load. Comparative studies are performed to demonstrate the accuracy and efficiency of the present theory. The gradients or inhomogeneities in materials play a vital role in determining the bending response of functionally graded material plates. The variation of material properties in the thickness direction can eliminate interface problems and thus the stress distributions are smooth. The analytical formulations and solutions presented herein should be useful in further studies and should provide engineers with the capability for the design of functionally graded material plates for advanced technical applications. Also, the present findings will be a useful benchmark for evaluating the other future plate theories and numerical methods, such as the finite element and meshless methods.

## References


[1] S.S. Vel, and R.C. Batra, "Exact solutions for thermoelastic deformations of functionally graded thick rectangular plates". *AIAA J*, Vol. **40 (**2002) 1421-1433.

[2] E. Reissner and Y.Stavsk, "Bending and stretching of certain types of heterogeneous aelotropic elastic plates". *ASME J ApplMech*, Vol. 28 (1961) 402-428.

[3] E. Reissner,"The effect of transverse shear deformation on the bending of elastic plates". *ASME J ApplMech*, Vol. **12 (1945) No. 2**, 69-77.

[4] R. D Mindlin," Influence of rotary inertia and shear on flexural motions of isotropic, elastic plates". *ASME J ApplMech*, Vol. **18 (**1951) 31-38.

[5] Huu-Tai Thai and ThucP.Vo, "A new sinusoidal shear deformation theory for bending, buckling, and vibration of functionally graded paltes". *Appl Math Model*,Vol. **37 (**2013) 3269-3281.

[6] J.N. Reddy and C.D. Chin, "Thermomechanical analysis of functionally graded cylinders and plates". J Therm stress, Vol. 21(1998) No.6, 593-626.

[7] A.M. Zenkour, "A comprehensive analysis of functionally graded sandwich plates:Part-1-Deflection and stresses". Int J Solids Struct, Vol. 42(2005) No. 18-19, 5224-5242.

[8] A.M. Zenkour, "A comprehensive analysis of functionally graded sandwich plates:Part-2-Buckling and free vibration". Int J Solids Struct, Vol. 42 (2005) No. 18-19, 5243-5258.

[9] A.M. Zenkour"Generalized shear deformation theory for bending analysis of functionally graded plates". Appl Math Model,Vol. 30 (2006) No. 1, 67-84.

[10] T. Kant, D.R.J.Owen, and O. C Zienkiewicz,"A refined higher order C0 plate element". Computstruct, Vol. 15 (1982) No. 2, 177-183.

[11] B.N.Pandya, and T. Kant, "Higher-order shear deformable theories for flexure of sandwich plates-finite element evaluations". Int J solids Struct, Vol. 24 (1988) No. 12, 1267-1286.

[12] B.N.Pandya, and T. Kant, "Finite element analysis of laminated composite plates using a higher order displacement model". Compos SciTechnol,Vol. 32, (1988) No. 2, 137-155.

[13] T. Kant, and K. Swaminathan, "Analytical solutions for the static analysis of laminated composite and sandwich plates based on higher order refined theory". Composite struct, Vol. 56 (2002) No. 4, 329-344.

[14] T. Kant, and K. Swaminathan, "Analytical solutions for free vibration analysis of laminated composite and sandwich plates based on higher order refined theory". compositestruct, Vol. 53 (2001) No. 1, 73-85.

[15] Garg Ajay Kumar, KhareRakesh Kumar, Kant Tarun, "Higher order closed form solutions for free vibration of laminated composite and sandwich shells. J Sandwich struct Mater, Vol. 8 (2006) No. 3, 205-235.

[16] M. E. Golmakani, and M. Kadkhodayan, " Nonlinear bending analysis of annular FGM plates using higher order shear deformation plate theories". Composite struct,Vol. 93 (2011) 973-982.

[17] Hiroyuki Matsunaga, " Free vibration and stability of functionally graded plates according to a 2-D higher-order deformation theory". Composite struct, Vol. 82 (2008) 499-512.

[18] Hiroyuki Matsunaga, "Stress analysis of functionally graded plates subjected to thermal and mechanical loadings". Composite struct, Vol. 87 (2009) 344-357.

[19] Song Xiang and Gui-wen Kang, "A nth-order shear deformation theory for the bending analysis on the functionally graded plates". European Journal of Mechanics A/Solids,Vol. 37 (2013) 336-343.

[20] A.M.A. Neves, A.J.M. Ferreira, E.Carrera, M.Cinefra, C.M.C.Roque, R.M.N.Jorge, and C.M.M. Soares, "Free vibration analysis of functionally graded shells by a higher-order shear deformation theory and radial basis functions collocation, accounting for through-the-thickness deformations". European Journal of Mechanics A/Solids, Vol. 37 (2013) 24-34.

[21] J.N.Reddy, "A review of refined theories of laminated composite plates", Shock, Vib. Dig. Vol. 22 (199) 3-17.

[22] M. Mallikarjuna, T. Kant, "A Critical review and some results of recently developed refined theories of fibre reinforced laminated composites and sandwiches". Compos. Struct,Vol. 23 (1993) 293-312.

[23] L. Dahsin, L. Xiaoyu, "An overall view of laminate theories based on displacement hypothesis". J Composite materials,Vol.30 (1996) 1539-1561.

[24] A.M.A. Neves, A.J.M. Ferreira, E.Carrera, M.Cinefra, C.M.C.Roque ,, R.M.N. Jorge, and C.M.M. Soares, "Static, free vibration and buckling analysis of isotropic and sandwich functionally graded plates using a quasi-3D higher-order shear deformation theory and meshless technique". Compos: Part B, Vol. 44 (2013) 657-674.

[25] Mechab, Ismail.H.A. Atmane, HA.Belhadejand E.A. A. Bedia, "A two variable refined plate theory for the bending analysis of functionally graded plates". Act Mech Sin,Vol. 26 (2010) 941-949.

[26] J.L.Mantari and C.GuedesSoares, "A novel higher-order shear deformation theory with stretching effect for functionally graded plates". Composites: Part B, Vol. 45 (2013) 268-281.

[27] M.Touratier, "An efficient standard plate theory", Int. J. Eng. Sci. Vol. 29 (1991) 901-916.

[28] Victor Birman and Larry W. Byrd, "Modeling and Analysis of Functionally Graded Materials and Structures", Applied Mechanics Reviews, Vol. 60 (2007) September, 195-216.

[29] J. N. Reddy, "Analysis of functionally graded plates". International Journal for Numerical Methods in Engineering, Vol. 47 (2000) issue 1-3, 663-684.

[30] Z-Q. CHENG and R. C. BATRA, "Deflection relationships between the homogeneous Kirchhoff plate theory and different functionally graded plate theories". Arch. Mech, Vol. 52 (2000) No.1, 143-158.

[31] Z-Q. Cheng, R. C. Batra, "Exact correspondence between eigenvalues of membranes and functionally graded simply supported polygonal plates". Journal of Sound and vibration, Vol. 229 (2000) No.4, 879-895.

[32] Z.-Q. Cheng, R.C. Batra, "Three-dimensional thermoelastic deformations of a functionally graded elliptic plate, Composites: Part B". Vol. 31 (2000) 97–106.

[33] M Michael. Gasik, Baosheng Zhang, Omer Van der Biest, Jozef Vleugels, Guy Anné, Stijn Put, "Design and Fabrication of Symmetric FGM Plates". Materials Science Forum, Vols. 23-28 (2003) 423-425.

[34] Batra and B. M. Love, "Adiabatic shear bands in functionally, Graded materials". Journal of Thermal Stresses, Vol. 27 (2004) 1101-1123.

[35] L. F. Qian, R. C. Batra, L. M. Chen, "Analysis of cylindrical bending thermoelastic deformations of functionally graded plates by a meshless local Petrov–Galerkin method". Computational Mechanics, Vol. 33 (2004) 263–273.

[36] D.F. Gilhooley, R.C. Batra, J.R. Xiao , M.A. McCarthy, J.W. Gillespie Jr, "Analysis of thick functionally graded plates by using higher-order shear and normal deformable plate theory and MLPG method with radial basis functions". Composite Structures, Vol. 80 (2007) 539–552.

[37] Mohammad Talha and B N Singh, "Thermo-mechanical deformation behavior of functionally graded rectangular plates subjected to various boundary conditions and loadings". International Journal of Aerospace and Mechanical Engineering, Vol. 6 (2012) No.1, 14-25.

[38] Tahar Hassaine Daouadji AbdelazizHadj Henni, Abdelouahed Tounsi, and Adda Bedia El Abbes, "A New Hyperbolic Shear Deformation Theory for Bending Analysis of Functionally Graded Plates", Hindawi Publishing Corporation, Modelling and Simulation in Engineering, Vol. 2012, 1-10, doi:10.1155/2012/159806.

[39] Song Xiang, Gui-wen Kang, "A nth-order shear deformation theory for the bending analysis on the functionally graded plates". European Journal of Mechanics A/Solids, Vol. 37 (2013) 336-343.

[40] S. Suresh, A. Mortensen, "Fundamentals of functionally graded materials". 1st ed. London: IOM Communications; 1998.

[41] B.N. Pandya and T. Kant, "Finite element stress analysis of laminated composite plates using higher order displacement model". Compos Sci Technol, Vol. 32 (1988) 137–55.

[42] J.N. Reddy, "Energy principles and variational methods in applied mechanics". John Wiley & Sons Inc; 2002.